Joint Diseases and Related Surgery

Jt Dis Relat Surg
2024;35(2):i-vii

ORIGINAL ARTICLE

A comparative analysis of 3D bioprinted gelatin-hyaluronic acid-alginate scaffold and microfracture for the management of osteochondral defects in the rabbit knee joint

Mahmud Aydin, MD[1], Mesut Ok, MD[1], Mehmet Halis Cerci, MD[2], Ramazan Demirhan, PhD[3], Serkan Surucu, MD[4], Mahir Mahirogullari, MD[2]

[1]Department of Orthopedics and Traumatology, Haseki Training and Research Hospital, Istanbul, Türkiye
[2]Department of Orthopedics and Traumatology, Memorial Şişli Hospital, Istanbul, Türkiye
[3]Department of Bioengineering, Yıldız Technical University, Istanbul, Türkiye
[4]Department of Orthopaedics and Rehabilitation, Yale University, New Haven, USA

ABSTRACT

Objectives: This study aims to compare the radiological, biomechanical, and histopathological results of microfracture treatment and osteochondral damage repair treatment with a new scaffold product produced by the three-dimensional (3D) bioprinting method containing gelatin-hyaluronic acid-alginate in rabbits with osteochondral damage.

Materials and methods: A new 3D bioprinted scaffold consisting of gelatin, hyaluronic acid, and alginate designed by us was implanted into the osteochondral defect created in the femoral trochlea of 10 rabbits. By randomization, it was determined which side of 10 rabbits would be repaired with a 3D bioprinted scaffold, and microfracture treatment was applied to the other knees of the rabbits. After six months of follow-up, the rabbits were sacrificed. The results of both treatment groups were compared radiologically, biomechanically, and histopathologically.

Results: None of the rabbits experienced any complications. The magnetic resonance imaging evaluation showed that all osteochondral defect areas were integrated with healthy cartilage in both groups. There was no significant difference between the groups in the biomechanical load test (p=0.579). No statistically significant difference was detected in the histological examination using the modified Wakitani scores (p=0.731).

Conclusion: Our study results showed that 3D bioprinted scaffolds exhibited comparable radiological, biomechanical, and histological properties to the conventional microfracture technique for osteochondral defect treatment.

Keywords: Bioprinted, histopathological, microfracture, osteochondral defect, scaffold, Wakitani score.

Osteochondral defects are serious problems that can cause degenerative arthritis, if left untreated due to low regeneration capacity. Osteochondral defects due to trauma or inflammation often regenerate with fibrous cartilage.[1,2] Since the resulting fibrocartilage is biomechanically more unstable than hyaline cartilage, symptoms of degeneration progress when exposed to mechanical loads for a long time.[3] In recent years, joint restoration of articular cartilage and subchondral bone has become accepted in the treatment of osteochondral defects.[4,5]

Debridement and microfracture are the oldest and easiest treatment methods in the treatment of osteochondral defects. The main disadvantage is that the cartilage renewed with these methods has

Received: January 13, 2024
Accepted: February 17, 2024
Published online: March 21, 2024

Correspondence: Mahmud Aydin, MD. Haseki Eğitim ve Araştırma Hastanesi, Ortopedi ve Travmatoloji Kliniği, 34096 Fatih, İstanbul, Türkiye.

E-mail: mahmut_aydn@windowslive.com

Doi: 10.52312/jdrs.2024.1626

Citation: Aydin M, Ok M, Cerci MH, Demirhan R, Surucu S, Mahirogullari M. A comparative analysis of 3D bioprinted gelatin-hyaluronic acid-alginate scaffold and microfracture for the management of osteochondral defects in the rabbit knee joint. Jt Dis Relat Surg 2024;35(2):i-vii. Doi: 10.52312/jdrs.2024.1626.

fibrocartilage properties.[6] Autologous or allogeneic osteochondral transplants, autologous chondrocytes, and three-dimensional (3D) scaffolds enriched with platelet-rich plasma (PRP), platelet-rich fibrin (PRF), or mesenchymal stem cells are other treatment methods in the treatment of osteochondral defects.[7-9] The disadvantages of these treatments are the donor site morbidity of autologous osteochondral transplantation its inadequacy in large defects, and the immunological responses and infection risk of allogeneic osteochondral transplants.[6,10-12] In recent years, with the widespread use of three-dimensional (3D) bioprinting technologies, scaffolds produced have taken their place in the treatment of osteochondral defects.[9,13]

In the present study, we hypothesized that repairing the osteochondral defect with the help of a 3D bioprinted scaffold would yield superior treatment results compared to microfracture treatment. We, therefore, aimed to compare the radiological, biomechanical, and histopathological results of microfracture treatment and osteochondral damage repair treatment with a new scaffold product produced by the 3D bioprinting method containing gelatin-hyaluronic acid-alginate in rabbits with osteochondral damage.

MATERIALS AND METHODS

Ten young (14 weeks old), female New Zealand White rabbits (Japan SLC) weighing 2.2 to 2.5 kg were used. By randomization, it was determined which side of 10 rabbits would be repaired with a 3D bioprinted scaffold, and microfracture treatment was applied to the other knees of the rabbits. A computer-based random number table procedure was applied for randomization. Two groups were created according to the applied treatment: Group 1 was the microfracture treatment group and Group 2 was the osteochondral defect repair treatment group with a new 3D bioprinted scaffold.

3D bioprinted scaffold preparation

A total of 10 mL solution is made from the mixed solution containing 4% alginate, 5% gelatin B, and 1% hyaluronic acid. The solution is stirred for 2 h at 37°C. Drop 0.9 mL of 2% CaCl2 solution and wait for half an hour for the gel to cross-link. The prepared solution is loaded into the syringe. The syringe is inserted into the 3D printer. During printing, 15% CaCl2 solution is sprayed on the scaffold once in each layer. After the scaffold printing is completed, 20% CaCl2 solution is sprayed seven times on the scaffold at 10-min intervals. The scaffold, which is kept at +4°C for one day, is prepared with 95% ethanol and 33 mM EDC-15 mM NHS solution the next day. The scaffold is immersed in 15 mL of the prepared solution. For the crosslinking process, the scaffold is kept in the solution at 37°C for 24 h. The scaffold taken from the oven (37°C) is removed from the crosslinking solution and the sterilization processes are as follows: 10 min distilled water, 30 min pure ethanol - 15 min PBS (pH 7.4) (Figure 1).

Surgical procedure

Anesthesia and postoperative care of the animals during surgery were carried out by expert veterinarians. After xylazine and ketamine anesthesia and cefazolin prophylaxis, both hind legs of the animal were shaved sterile painted, and covered.

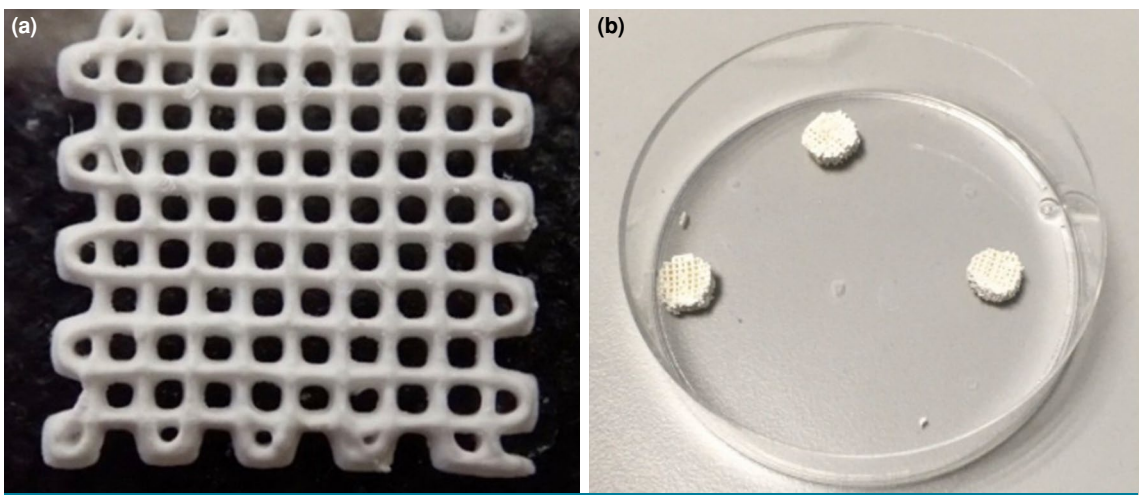

FIGURE 1. Image of a new three-dimensional bioprinted scaffold consisting of gelatin, hyaluronic acid and alginate designed by us.

The knee joint was palpated and entered through a midline incision. After passing the skin below the pelvis, the medial parapatellar incision was made from the medial side of the patella. The patella was tipped laterally and the patellofemoral groove was reached. Then, a full-thickness osteochondral defect with a width of 5 mm and a depth of 6 mm was created using a mosaicplasty set in the patellofemoral groove. In Group 1, microfracture treatment was applied without repairing the defect (Figure 2a). Afterward, the extensor mechanism was repaired and the subcutaneous and skin were closed. In Group 2, the defect was repaired with the help of a 3D bioprinted scaffold (Figure 2b). After the defect reached the same level as the intact adjacent cartilage, the patella was reduced and the osteochondral fragment was covered. The extensor mechanism was repaired. The subcutaneous tissue and skin were closed. Dressing was done. Cefazolin prophylaxis of the animals was continued for 24 h. They were allowed to move freely in their cages with access to water and feed. The animals were followed for about six months.

Radiological evaluation

Bilateral knee magnetic resonance imaging (MRI) was performed on each anesthetized animal before sacrifice. A 3 Tesla Siemens screw XQ MRI device was used. (Coil: Knee Coil 18 channels Siemens). Thin sections of 2 mm were taken. Samples were acquired with a repetition time of 35 ms, an echo time of 19 ms (effective), a field of view (Fov) of 121×148, and an acquisition time (TA) of 3.54. A personalized knee protocol was applied to all samples using a cartilage-sensitive fast spin echo sequence in the sagittal plane. The MRI evaluation was performed by a single-blinded radiologist according to the MRI Magnetic Resonance Observation of Cartilage Repair Tissue (MOCART) scoring system for all samples.[14]

Biomechanical evaluation

The samples were placed in a phosphate-based solution and kept at room temperature for 3 h, and the samples were placed on the metal surface perpendicular to the end of the cylindrical indentation with a diameter of 2 mm. The samples were kept moist throughout the experiment. A texture analyzer called Stable Microsystems (Instron Model 3365, Instron Engineering Corporation, Norwood, MA, USA) was used. A compression test was applied. Stress-strain graphs were drawn, and the load at which the cartilage and subchondral bone broke under continuous compression and the strain values at this value were compared (Figure 3).

Histological evaluation

All animals were sacrificed six months after transplantation. Extracted tissues were fixed in

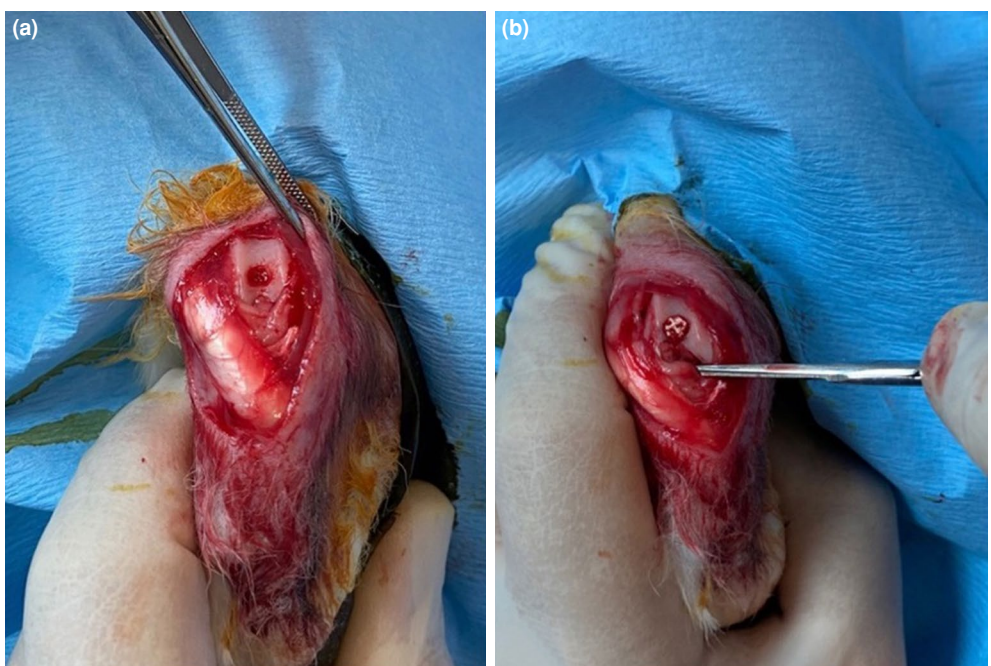

FIGURE 2. Images of surgical procedures. **(a)** Creating a 5-mm wide and 6-mm deep full-thickness osteochondral defect in the patellofemoral groove. **(b)** Repair of the osteochondral defect created in the patellofemoral groove with a three-dimensional bioprinted scaffold.

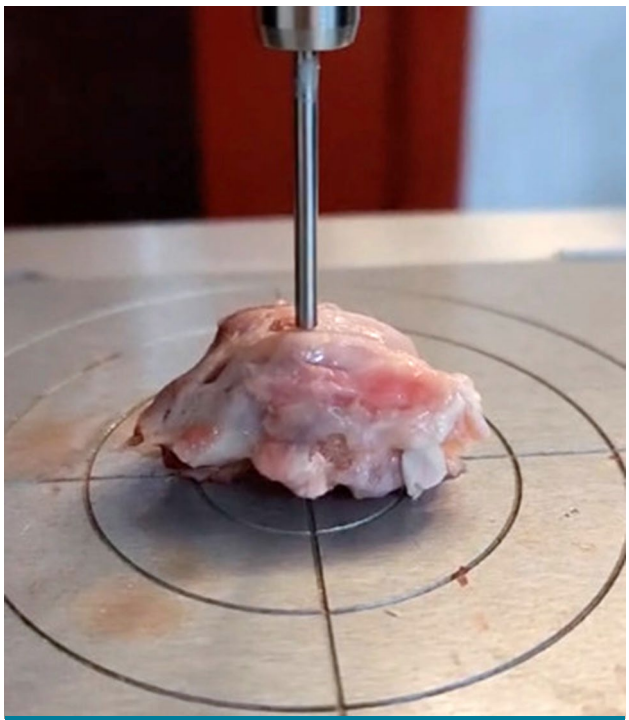

FIGURE 3. Biomechanical load test image with Stable Microsystems.

10 times the volume of 10% buffered formaldehyde for at least 24 h. The samples were monitored for 12 h on the automatic tissue device. Then, it was turned into paraffin blocks. Slide sections with a thickness of 3 to 4 microns were taken from paraffin blocks. Following deparaffinization, routine hematoxylin and eosin (H&E) and Safranin-0 staining was applied. Each slide was cover slipped using Entellan™ (Merck KGaA, Darmstadt, Germany). Samples were evaluated by a blinded histologist according to the modified Wakitani Histological scoring.[4]

Statistical analysis

Power analysis and sample size calculation were performed using the G*power version 3.1 software (Heinrich-Heine-Universität Düsseldorf, Düsseldorf, Germany). The effect size, the alpha, and the power (1-beta) were used to estimate the required sample size. These were 2.18, 0.05, and 0.95, respectively. We used 10 samples for each group.[13,15]

Statistical analysis was performed using the NCSS version 2020 software (NCSS LLC., Kaysville, UT, USA). Descriptive data were presented in mean ± standard deviation (SD), median (min-max) or number and frequency, where applicable. The independent sample t-test was used for two group comparisons. The Pearson chi-square test was used to compare qualitative data. *P* values of <0.01 and <0.05 were considered statistically significant.

RESULTS

Radiological results

According to the MOCART scoring system, the average score was 94.20 in the microfracture treatment group and 95.80 in the scaffold-assisted group. There was no statistically significant

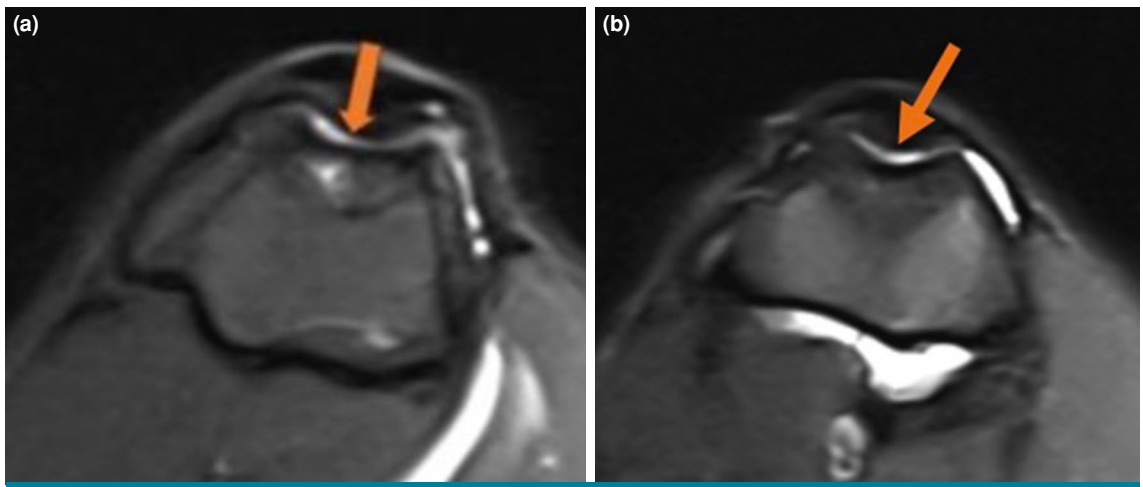

FIGURE 4. Axial MRI images six months after osteochondral defect repair. **(a)** Axial MRI images six months after microfracture treatment. **(b)** Axial MRI images six months after osteochondral defect repair treatment with a new three-dimensional bioprinted scaffold.
MRI: Magnetic resonance imaging.

difference between the groups (p=0.757). No cartilage defect was observed in either group. Subchondral bone and cartilage continuity was normal in both groups. The cartilage surfaces were found to be intact. The signal intensity of the cartilage tissue formed in the defective areas was the same in both groups (Figure 4).

Biomechanical results

Biomechanically, maximum stress measurements at the time of load did not show a statistically significant difference (p=0.579). In addition, maximum strain values at load did not show a statistically significant difference according to the groups (p=0.731) (Table I).

Histopathological results

According to the histopathological examination performed according to the modified Wakitani scoring system, cell morphology (p=0.877), matrix staining with Safranin-O and fast green (p=0.890), cartilage thickness (p=0.809), implantation with adjacent host cartilage (p=0.500), and Wakitani total scores (p=0.190), no significant difference was observed between the two groups (Tables 2 and 3) (Figures 5 and 6).

TABLE I
Evaluation of biomechanical measurement results of both groups

	Group 1			Group 2			
	Mean±SD	Median	Min-Max	Mean±SD	Median	Min-Max	*p*
Max-load stress (MPa)	68.33±35.00	76.27	17.69-120.20	62.31±32.11	70.58	10.55-102.10	0.579
Max-load strain (MPa)	43.15±10.96	37.77	35.76-64.30	41.22±13.59	37.79	26.40-68.70	0.731

Mann-Whitney U test.

TABLE II
Evaluation of histological modified Wakitani score measurements according to groups

	Group 1 (n=10)	Group 2 (n=10)	
	n	n	*p*
Cell morphology			0.877
Hyaline cartilage	2	3	
Mostly hyaline cartilage	3	3	
Mostly fibrocartilage	3	2	
Mostly noncartilage	1	2	
Noncartilage	0	0	
Matrix staining with Safranin-O and fast green			0.890
Normal (compared with host adjacent cartilage)	3	4	
Slightly reduced (%)	6	5	
Markedly reduced (%)	1	1	
No metachromatic stain	0	0	
Thickness of cartilage (mm)			0.809
>2/3	5	6	
1/3-2/3	3	3	
<1/3-2/3	2	1	
Integration of implant with adjacent host cartilage			0.500
Both edges integrated	8	9	
One edge integrated	2	1	
Neither edge integrated	0	0	

Pearson chi-square.

TABLE III
Evaluation of histological results of both groups according to Modified Wakitani Total Score

	Group 1			Group 2			
	Mean±SD	Median	Min-Max	Mean±SD	Median	Min-Max	*p*
Modified Wakitani Total Score	2.90±1.19	3	1-5	2.30±0.94	2	1-4	0.190

Mann-Whitney U test.

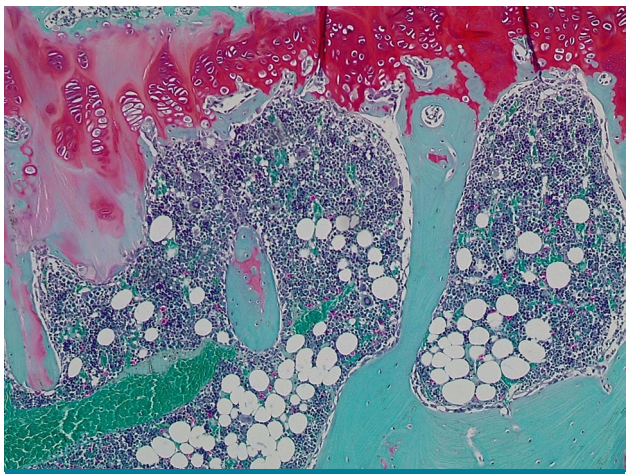

FIGURE 5. Histopathological examination of the injured articular cartilage using hematoxylin-eosin staining at various time points after microfracture treatment (×100).

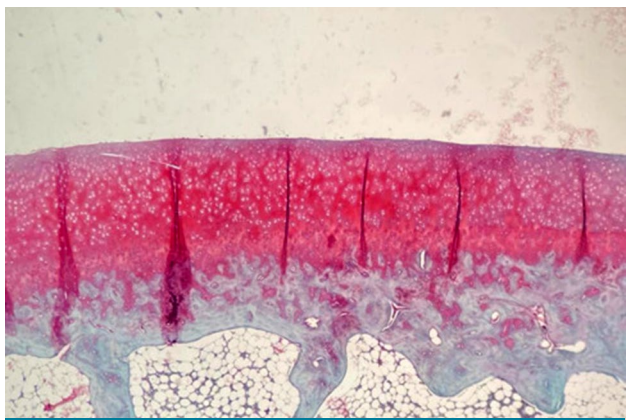

FIGURE 6. Histopathological examination of the injured articular cartilage using hematoxylin-eosin staining at various time points after osteochondral defect repair treatment with a new three-dimensional bioprinted scaffold (×100).

DISCUSSION

The treatment of osteochondral defects is a critical challenge in orthopedic medicine due to the limited regenerative capacity of articular cartilage. In the present study, we performed a comprehensive evaluation of two distinct methods for treating osteochondral lesions in a rabbit model, comparing the outcomes of a 3D bioprinted scaffold and traditional microfracture treatment. The results showed no significant histological or biomechanical differences between the two groups. Additionally, there were no significant disparities on MRI imaging, indicating comparable effectiveness in both treatment approaches.

While treating chondral and osteochondral defects, the main goal is to achieve effective results with low cost, low morbidity, single-stage surgery, early mobilization, and long-term effectiveness. Osteochondral allograft transplantation carries considerable risks, limited utility, and considerable costs. Similarly, autologous chondrocyte implantation and matrix-associated autologous chondrocyte implantation require two-stage procedures, making them expensive and complex. To overcome these limitations, researchers have focused on scaffold-based approaches, which offer the advantage of single-stage application in osteochondral defects, including the subchondral bone.[16,17] In the current study, 3D bioprinted scaffolds were used, and they showed promising histopathological outcomes. The scaffold, manufactured through 3D printing technology, facilitated the formation of hyaline cartilage tissue after osteochondral defect repair. This approach provides a potential alternative to traditional methods by combining the benefits of scaffold-based treatments with the advantages of 3D printing technology.

An important aspect of this study was the variety of materials used in the production of osteochondral scaffolds in the literature.[13,16] Yang et al.[13] used a scaffold composed of alginate and hydroxyapatite to treat osteochondral defects in rabbits, ultimately observing hyaline-like cartilage formation. Xue et al.[16] developed a scaffold using polylactide-co-glycolide and nano-hydroxyapatite, resulting in hyaline-like cartilage formation in the rabbit model. This study follows these approaches, offering comparable and promising results through the use of a scaffold created with 3D bioprinting technology. The presence of gelatin in the scaffold is of particularly crucial,

as it serves as a robust matrix for cellular adhesion. Complementing this effect, hyaluronic acid actively promotes cell migration and proliferation within the damaged region, further enhancing tissue regeneration. The innovative approach employed in this study involved the creation of a porous scaffold structure, enabling efficient cell dispersion throughout the implant by leveraging advanced 3D bioprinting techniques. This strategic integration of gelatin, hyaluronic acid, and cutting-edge bioprinting techniques holds great promise for advancing tissue engineering, offering a groundbreaking solution to enhance cellular therapies and tissue regeneration.

Nonetheless, this study has both strengths and limitations. One of its strengths was that it evaluated the results of two different treatment methods radiologically, biomechanically, and histopathologically. However, the main limitations to this study are that the number of subjects in both groups was relatively small and the radiological results were evaluated by a single radiologist.

In conclusion, 3D bioprinted scaffolds enriched with gelatin, hyaluronic acid, and alginate have been shown to exhibit radiological, biomechanical, and histological properties comparable to the conventional microfracture technique for osteochondral defect treatment. Additionally, the gelatin, hyaluronic acid, and alginate-enriched scaffold was found to be biocompatible, biodegradable, and able to promote cartilage regeneration and repair in the *in vivo* animal model.

Ethics Committee Approval: The study protocol was approved by the Marmara University Animal Experiments Local Ethics Committee (date: 14.12.2021, no: 99.2021mar). The study was conducted in accordance with the principles of the Declaration of Helsinki.

Data Sharing Statement: The data that support the findings of this study are available from the corresponding author upon reasonable request.

Author Contributions: Idea/concept: M.M., M.H.C.; Design: M.A., M.O.; Data collection/processing: M.A., M.H.C.; Analysis/interpretation: S.S., M.A.; Literature review: R.D., M.A., Drafting/writing: M.O., M.H.C., M.A.; Critical review: M.A., S.S., M.M.

Conflict of Interest: The authors declared no conflicts of interest with respect to the authorship and/or publication of this article.

Funding: The authors received no financial support for the research and/or authorship of this article.

REFERENCES

1. Uzun E, Güvercin S, Günay AE, Kafadar İH, Bolat D, Yay AH, et al. The effect of oral hydroxychloroquine on chondral defect: An experimental study. Jt Dis Relat Surg 2023;34:628-39. doi: 10.52312/jdrs.2023.1114.
2. Baghaban Eslaminejad M, Malakooty Poor E. Mesenchymal stem cells as a potent cell source for articular cartilage regeneration. World J Stem Cells 2014;6:344-54. doi: 10.4252/wjsc.v6.i3.344.
3. Kekeç AF, Yıldırım A. Mid-term results of autologous matrix-induced chondrogenesis surgery with or without scaffolds for arthroscopic treatment of deep talus osteochondral lesions: A comparative study. Jt Dis Relat Surg 2023;34:613-9. doi: 10.52312/jdrs.2023.1197.
4. Wakitani S, Goto T, Pineda SJ, Young RG, Mansour JM, Caplan AI, et al. Mesenchymal cell-based repair of large, full-thickness defects of articular cartilage. J Bone Joint Surg [Am] 1994;76:579-92. doi: 10.2106/00004623-199404000-00013.
5. Szerb I, Hangody L, Duska Z, Kaposi NP. Mosaicplasty: Long-term follow-up. Bull Hosp Jt Dis 2005;63:54-62.
6. Mithoefer K, McAdams T, Williams RJ, Kreuz PC, Mandelbaum BR. Clinical efficacy of the microfracture technique for articular cartilage repair in the knee: An evidence-based systematic analysis. Am J Sports Med 2009;37:2053-63. doi: 10.1177/0363546508328414.
7. Brittberg M, Lindahl A, Nilsson A, Ohlsson C, Isaksson O, Peterson L. Treatment of deep cartilage defects in the knee with autologous chondrocyte transplantation. N Engl J Med 1994;331:889-95. doi: 10.1056/NEJM199410063311401.
8. Georgi N, van Blitterswijk C, Karperien M. Mesenchymal stromal/stem cell-or chondrocyte-seeded microcarriers as building blocks for cartilage tissue engineering. Tissue Eng Part A 2014;20:2513-23. doi: 10.1089/ten.TEA.2013.0681.
9. Bahadır B, Atik OŞ, Kanatlı U, Sarıkaya B. A brief introduction to medical image processing, designing and 3D printing for orthopedic surgeons. Jt Dis Relat Surg 2023;34:451-4. doi: 10.52312/jdrs.2023.57912.
10. Garretson RB 3rd, Katolik LI, Verma N, Beck PR, Bach BR, Cole BJ. Contact pressure at osteochondral donor sites in the patellofemoral joint. Am J Sports Med 2004;32:967-74. doi: 10.1177/0363546503261706.
11. Ahmad CS, Cohen ZA, Levine WN, Ateshian GA, Mow VC. Biomechanical and topographic considerations for autologous osteochondral grafting in the knee. Am J Sports Med 2001;29:201-6. doi: 10.1177/03635465010290021401.
12. Ghazavi MT, Pritzker KP, Davis AM, Gross AE. Fresh osteochondral allografts for post-traumatic osteochondral defects of the knee. J Bone Joint Surg [Br] 1997;79:1008-13. doi: 10.1302/0301-620x.79b6.7534.
13. Yang Y, Yang G, Yongfei S, Xu Y, Zhao S, Wenyuan Z. 3D bioprinted integrated osteochondral scaffold-mediated repair of articular cartilage defects in the rabbit knee. J Med Biol Eng 2020;40:71-81. doi: 10.1007/s40846-019-00481-y.
14. Goebel L, Zurakowski D, Müller A, Pape D, Cucchiarini M, Madry H. 2D and 3D MOCART scoring systems assessed by 9.4 T high-field MRI correlate with elementary and complex histological scoring systems in a translational model of osteochondral repair. Osteoarthritis Cartilage 2014;22:1386-95. doi: 10.1016/j.joca.2014.05.027.
15. Yamaguchi S, Aoyama T, Ito A, Nagai M, Iijima H, Tajino J, et al. The effect of exercise on the early stages of mesenchymal stromal cell-induced cartilage repair in a rat osteochondral defect model. PLoS One 2016;11:e0151580. doi: 10.1371/journal.pone.0151580.
16. Xue D, Zheng Q, Zong C, Li Q, Li H, Qian S, et al. Osteochondral repair using porous poly(lactide-co-glycolide)/nano-hydroxyapatite hybrid scaffolds with undifferentiated mesenchymal stem cells in a rat model. J Biomed Mater Res A 2010;94:259-70. doi: 10.1002/jbm.a.32691.